Concurrent Expression of Erythroid and Renal Aquaporin CHIP and Appearance of Water Channel Activity in Perinatal Rats

Barbara L. Smith,* Ruben Baumgarten,* Søren Nielsen,‡ Daniel Raben,* Mark L. Zeidel,§ and Peter Agre*

**Departments of Medicine, Biological Chemistry, Cell Biology/Anatomy, and Physiology, Johns Hopkins University School of Medicine, Baltimore, Maryland 21205; ‡Department of Cell Biology, Institute of Anatomy, University of Aarhus, DK-8000 Aarhus C, Denmark; §Research Service, West Roxbury Department of Veterans Affairs Medical Center, West Roxbury, Massachusetts 02132; and Department of Medicine, Brigham and Women's and Children's Hospitals, Harvard Medical School, Boston, Massachusetts 02115*

Abstract

Major phenotypic changes occur in red cell membranes during the perinatal period, but the underlying molecular explanations remain poorly defined. Aquaporin CHIP, the major erythroid and renal water channel, was studied in perinatal rats using affinity-purified anti-CHIP IgG for immunoblotting, flow cytometry, and immunofluorescence microscopy. CHIP was not detected in prenatal red cells but was first identified in circulating red cells on the third postnatal day. Most circulating red cells were positive for CHIP by the seventh postnatal day, and this proportion rose to nearly 100% by the 14th day. The ontogeny of red cell CHIP correlated directly with acquisition of osmotic water permeability and inversely with Arrhenius activation energy. Only minor alterations in the composition of red cell membrane lipids occurred at this time. Immunohistochemical analysis of perinatal kidneys demonstrated a major induction of CHIP in renal proximal tubules and descending thin limbs at birth, coincident with the development of renal concentration mechanisms. Therefore, water channels are unnecessary for oxygen delivery or survival in the prenatal circulation, however CHIP may confer red cells with the ability to rehydrate rapidly after traversing the renal medulla, which becomes hypertonic after birth. (*J. Clin. Invest.* 1993. 92:2035–2041.)

Key words: fetal blood • erythrocyte membrane • kidney tubules • cell membrane permeability • water movements

Introduction

Adult human red cells differ markedly from fetal red cells, which contain fetal isoforms of hemoglobin and glycolytic enzymes, and fetal patterns of blood group antigens (see reviews in references 1 and 2). Fetal red cells have reduced survival times in the circulation and are significantly larger than adult red cells. Although most fetal red cell membrane transport pathways resemble adult, membrane [^{3}H]water permeability is reduced (3).

Channel-forming integral membrane protein (CHIP)[1] is a 28-kD integral membrane protein (4–6) that is the first known molecular water channel (7). CHIP is the archetypal member (human genome symbol AQP1) of a family of plant and mammalian water transporters now referred to as the "aquaporins" (8). CHIP forms the major water transport pathway of red cells (9) and renal proximal tubules and descending thin limbs (10), a role that has been confirmed and further defined by other laboratories (see review in reference 11). Of note, only a single CHIP gene (12) is expressed in several water-permeable epithelia throughout the body (13–15).

It remains unexplained why fetal red cells have reduced water permeability, although a reduced number of membrane water channels is possible. It also remains unexplained why red cells should need water channels, since oxygen delivery and survival in the circulation are apparently unrelated to transmembrane water movement (16). In situ hybridizations of fetal rats revealed surprisingly complex patterns of CHIP expression: choroid plexus contained CHIP mRNA throughout life; fetal cornea expressed the transcript transiently; erythroid tissues and kidneys expressed negligible CHIP mRNA until after birth (17). This study was undertaken to document the expression of aquaporin CHIP protein in perinatal rat red cells and kidneys in conjunction with biophysical studies of red cell membrane water permeability.

Methods

Materials. Affinity-purified polyclonal rabbit antibodies to the 4-kD cytoplasmic domain of human red cell CHIP and nonimmune rabbit IgG were described (5, 10). Affinity-purified polyclonal rabbit antibodies to human red cell spectrin and anion exchanger-band 3 were obtained from Vann Bennett (Duke University Medical Center, Durham, NC). Reagents and other supplies were from Baker Co. (Sanford, ME), Bio-Rad Laboratories (Richmond, CA), or Sigma Immunochemicals (St. Louis, MO).

Rat red cells. Timed pregnant Sprague Dawley rats were from Harlan Sprague Dawley Inc. (Indianapolis, IN). Pregnant rats and rat pups were anesthetized by CO_2 inhalation and decapitated according to Johns Hopkins- and Harvard-approved protocols. Prenatal rats were removed from the uterus, thoroughly rinsed with saline to remove all maternal red cells, and decapitated. Peripheral blood was collected in petri dishes containing chilled PBS (0.15 M NaCl and 7.5 mM sodium

This work was presented in part at the annual meeting of the American Association for Clinical Investigation, Washington DC, May 1, 1993 (*Clin. Res.* 1993 41:206. [Abstr.]).

Address correspondence to Dr. Peter Agre, Johns Hopkins University School of Medicine, 725 North Wolfe Street, Baltimore, MD.

Received for publication 4 May 1993 and in revised form 20 July 1993.

1. *Abbreviations used in this paper:* CHIP, channel-forming integral membrane protein; E_a, Arrhenius activation energy; P_f, coefficient of osmotic water permeability.

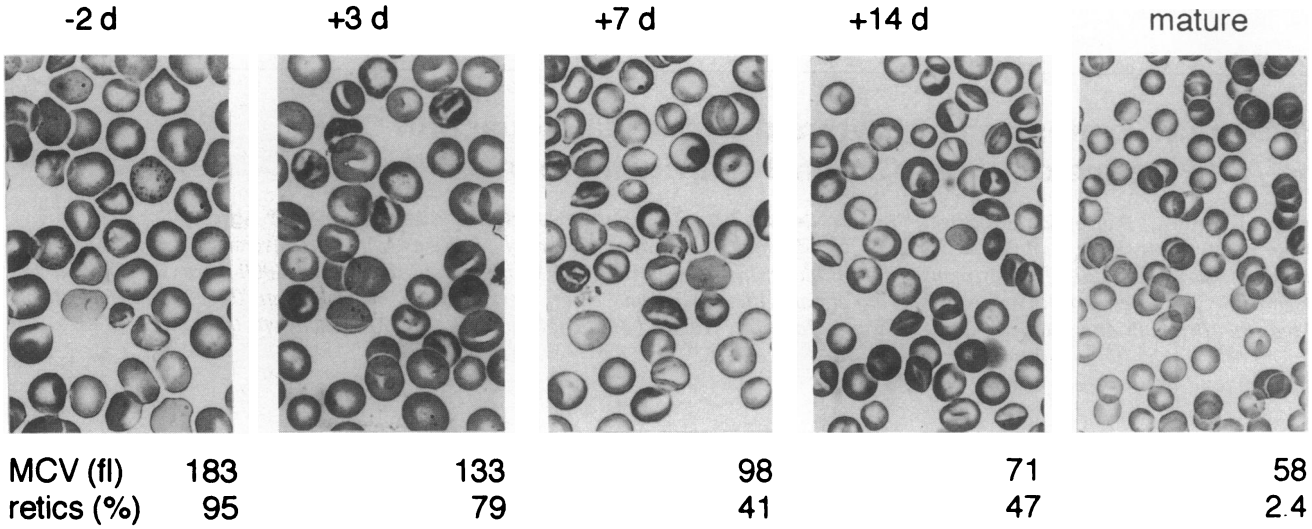

Figure 1. Peripheral blood from prenatal and neonatal rats of indicated ages were stained with Wright's reagent (×650). The mean corpuscular volumes and percentage of reticulocytes are listed.

phosphate, pH 7.4) and 1 mM NaEDTA. Red cell indices and peripheral blood smears were processed in the clinical hematology laboratories at Johns Hopkins Hospital and the West Roxbury Veterans Administration Medical Center by routine procedures. Reticulocyte counts of 1,000 cells per sample were visually counted after new methylene blue staining. Red cells were washed by low-speed centrifugation in chilled PBS, and membranes were prepared by lysis in 7.5 mM sodium phosphate (pH 7.4), 1 mM NaEDTA, 4 μg/ml leupeptin, 0.2 mM phenylmethylsulfonyl fluoride, 0.5 mg/ml diisopropylfluorophosphate, and high-speed centrifugation (18). SDS-PAGE and immunoblotting of 12% acrylamide 0.7 × 7 × 9 cm slabs (19), and enhanced chemiluminescence (Amersham Corp., Arlington Heights, IL) were described (10).

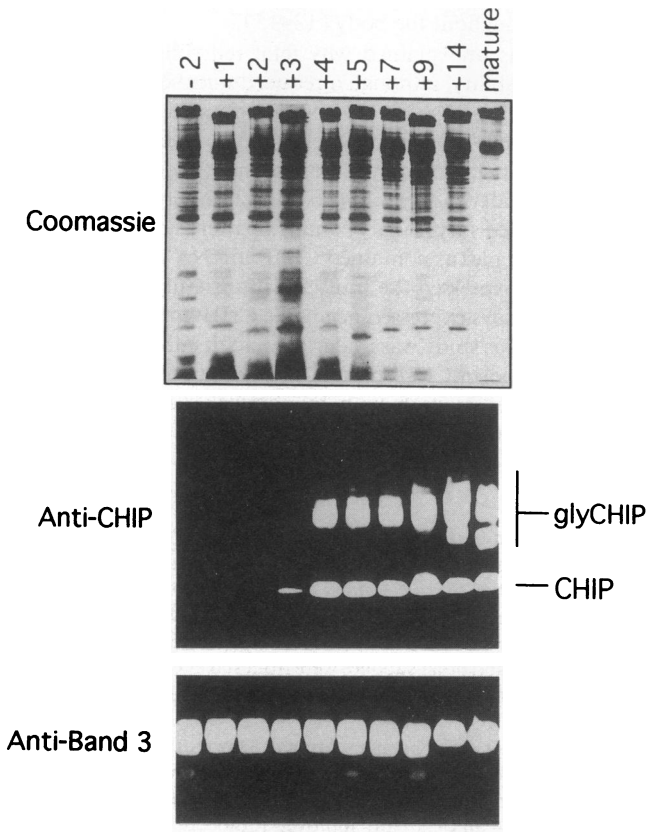

Figure 2. Expression of aquaporin CHIP in red cell membranes determined by immunoblot. (*Top*) Coomassie blue–stained SDS-PAGE slab of membranes (3–10 μg protein/lane) from peripheral blood of rats of defined ages. The photo is the composite of a series of 12% acrylamide gels run separately on membrane samples immediately after their preparation. (*Middle* and *bottom*) Anti-CHIP and anti–band 3 immunoblots of the same membrane samples processed en bloc.

Immunofluorescence microscopy. Membranes prepared from rat red cells were suspended to 10 vol in PBS containing 3% paraformaldehyde and incubated 15 min at room temperature. The membranes were settled for 10 min upon poly-L-lysine–coated coverslips, washed three times with PBS, incubated 30 min with 50 mM NH_4Cl in PBS, and washed three more times in PBS. The membranes were permeabilized by a 15-min incubation in 0.1% Triton X-100 in PBS, and then incubated 20 min and washed twice with 10% FBS in PBS. The coverslips were then sequentially covered with the following agents in 50 μl FBS-PBS: (*a*) anti-CHIP, 0.1 μg, 45 min; (*b*) FITC-conjugated goat anti–rabbit IgG (Boehringer Mannheim, Corp., Indianapolis, IN), 2.5 μg, 20 min; (*c*) antispectrin, 0.2 μg, 45 min; and (*d*) Texas red–conjugated goat anti–rabbit IgG (Jackson Immunoresearch Labs, Inc., West Grove, PA), 0.4 μg, 20 min. Four FBS-PBS washes followed each step. Coverslips were mounted with 0.1 M *N*-propylgallate in glycerol before microscopy (Nikon Microphot, Melville, NY) and photography using filters compatible with FITC or Texas red and Kodak Tri-X pan 400 film.

Flow cytometry. Approximately 20 μl of red cell membranes was washed three times by dilution to 1 ml in PBS followed by 5-min, 2°C centrifugations at 1,000 *g*. The membranes were fixed for 15 min at room temperature in 500 μl 0.5% paraformaldehyde in PBS, washed three times in PBS, permeabilized for 15 min in 500 μl 0.1% Triton X-100 in PBS-BSA (4% BSA), and washed three times in PBS-BSA. The membranes were resuspended to 50 μl and incubated for 1 h at 4°C with 0.03 μg nonimmune rabbit IgG or anti-CHIP, then washed three times with PBS-BSA. The membranes were then incubated similarly with 2 μg FITC-conjugated goat anti–rabbit IgG, and washed once with PBS-BSA and twice with PBS. Fluorescence levels were detected with a flow cytometer (FACScan®; Becton Dickinson Instruments, Inc., Fullerton, CA). Data were accumulated on gated membrane particles and analyzed with FACScan® Research Software.

Measurement of red cell osmotic water permeability. Methods were adapted from our previous report (9). Coefficient of osmotic water permeability (P_f) was measured by abruptly doubling the osmolality

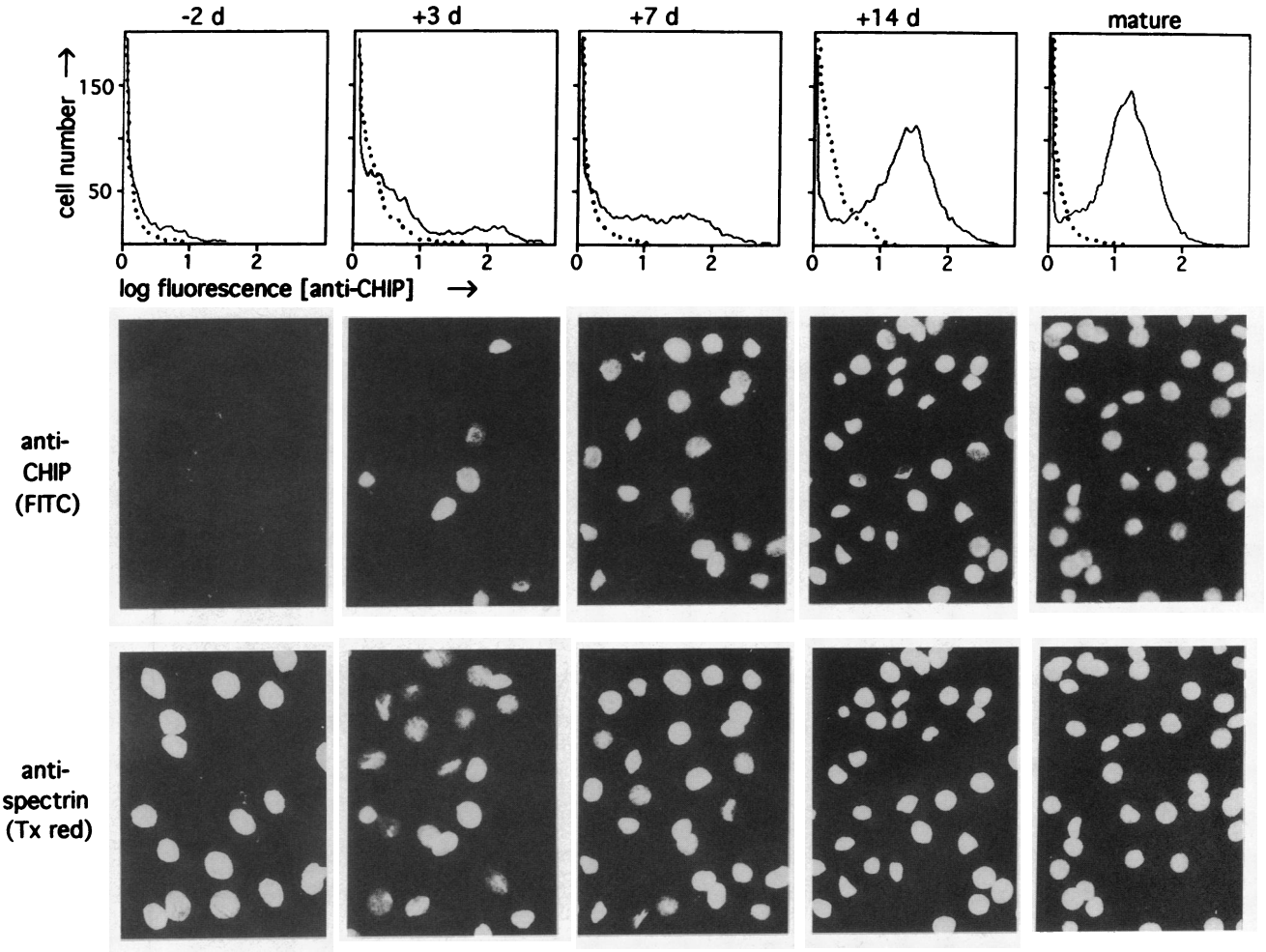

Figure 3. Red cell membranes from rats of defined ages analyzed by immunofluorescence with anti-CHIP. (*Top*) Flow cytometry of aliquots of permeabilized membranes after incubation with preimmune IgG followed by FITC-goat anti-rabbit IgG (*dotted lines*) or anti-CHIP, followed by FITC-goat anti-rabbit IgG (*solid lines*). Each histogram represents fluorescence of 10,000 membrane particles. (*Middle* and *bottom*) Immunofluorescence microscopy of permeabilized membranes after sequential incubations: anti-CHIP; FITC-goat anti-rabbit IgG; antispectrin; and Texas red-goat anti-rabbit IgG. Optical filters were used to separately visualize anti-CHIP-positive red cells (FITC) or all red cells (antispectrin-Texas red) in the same field.

surrounding intact red cells with an equal volume of PBS-sucrose by stopped flow fluorimetry, dead time of 0.9 ms (SF.17MV; Applied Photophysics, Leatherhead, United Kingdom). Red cell volumes were monitored by light scattering: excitation wavelength = 600±1.5 nm, generated with a 150-W mercury-xenon arc lamp and monochrometer, f3.4 grating (Applied Photophysics); emission wavelength > 515 nm was measured through a cut-on filter (Oriel Corp., Stratford, CT). Red cells acted as perfect osmometers over the osmolalities tested; relative volume (absolute/initial) was inversely related to relative signal (absolute/initial). Averaged data from 8–16 determinations were fit to single exponential curves (9). Fitting parameters were used to determine P_f by applying linear conversion from relative fluorescence to relative volume and iteratively solving with software (MathCAD; MathSoft, Cambridge, MA):

$$dV(t)/dt = (P_f) \times (SAV) \times (MVW) \times [(C_{in}/V(t)) - C_{out}], \quad \text{(equation 1)},$$

where $V(t)$ is relative red cell volume as a function of time, P_f in cm/s, SAV is the vesicle surface area/volume ratio, MVW is the molar volume of water (18 ml/mol), and C_{in} and C_{out} are the initial concentrations of total solute inside and outside the cell. Red cell radii were calculated from cell volume.

Membrane lipid studies. These methods were previously described (20).

Rat kidneys. Pregnant rats and postnatal rat pups were heparinized, anesthetized with pentobarbital, and fixed by vascular perfusion through the left ventricle after incision of the right auricle (modified from Larsson, reference 21). The fixative contained 8% paraformaldehyde in 0.1 M Na cacodylate buffer (pH 7.2); tissue blocks from cortex, outer, and inner medulla were postfixed for an additional 2 h, cryprotected in 2.3 M sucrose containing 2% paraformaldehyde for 30 min, mounted on holders, and rapidly frozen in liquid N_2. Immunolabeling was performed on 0.85-μm cryosections with anti-CHIP (0.15 μg/ml), visualized with horseradish peroxidase-conjugated goat anti-rabbit IgG, and counterstained with Mayer's hematoxylin (10). Specificity of immunolabeling was confirmed with nonimmune rabbit IgG, incubation without primary antibody, or preadsorption of anti-CHIP with a molar excess of pure CHIP (10).

Results and Discussion

Perinatal red cell morphology. Red cells changed progressively during the first 2 wk of postnatal life. Red cells from prenatal rats were three times larger than red cells from mature rats (−2

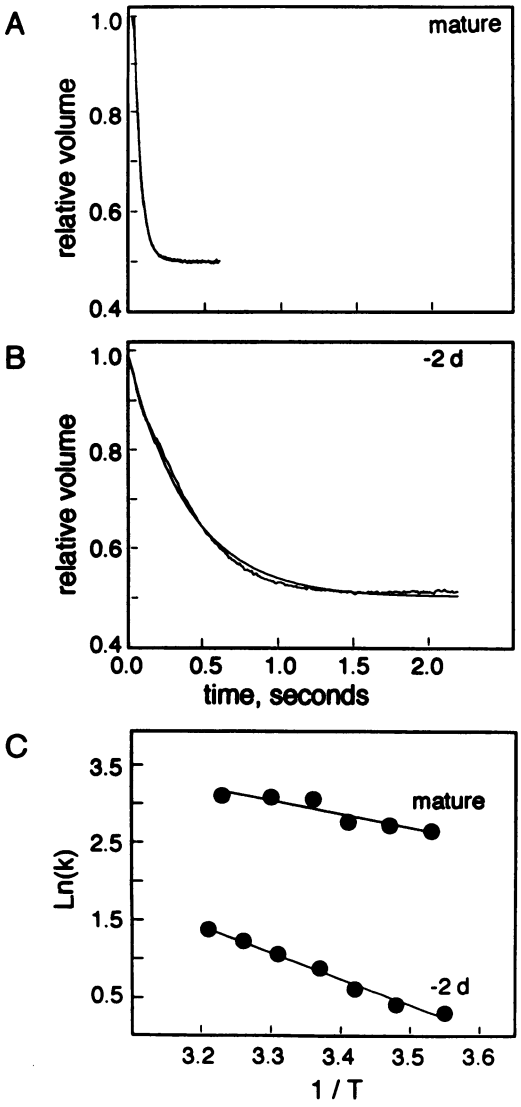

Figure 4. Water permeability of prenatal and adult red cells. Volumes of red cells from rats of defined ages were measured by light scattering after abruptly increasing the extracellular osmolality by 100%. (*A* and *B*) Change in volume with time measured at 23°C. Representative data and fitted single exponentials are shown. (*C*) Arrhenius plot of determinations at 8–39°C. Ordinate represents the natural logarithm of the rate constant, k (U = 1/s) derived from the fitted single exponential describing the time course of water efflux. Abscissa represents 1,000× the reciprocal of the temperature (°K).

d; Fig. 1). Prenatal red cells were frequently stippled and contained intense polychromatophilia with reticulocyte counts approaching 100%. A second population of smaller red cells appeared after birth (+3 d; Fig. 1) and progressively replaced the larger cells (+14 d; Fig. 1). Although declining, the percentage of reticulocytes remained > 40% throughout the postnatal period.

Expression of aquaporin CHIP in perinatal red cells. When analyzed by Coomassie-stained SDS-PAGE, the red cell membrane proteins of prenatal and postnatal rats resembled those of mature rats with respect to abundance and mobility of spectrin, anion exchanger-band 3, bands 4.1 and 4.2, and actin (Fig. 2). Perinatal red cell membranes at all stages also had increased membrane-associated globin. Several other membrane proteins, including bands 6, 7, and 8, were increased, but no Coomassie-stained membrane protein was missing.

Since it fails to stain with Coomassie, CHIP was evaluated in perinatal red cell membranes by anti-CHIP immunoblot. CHIP first appeared at +3 d and progressively increased in abundance over the next 4 d. Appearance of CHIP at this developmental point was observed in all rat pups from multiple litters born on four different occasions. The electrophoretic mobility of the glycosylated subunit changed from a narrow band (+4 d; Fig. 2) to a broader band in subsequent days (+7 to +14 d), consistent with increased heterogeneity of the complex oligosaccharide (22).

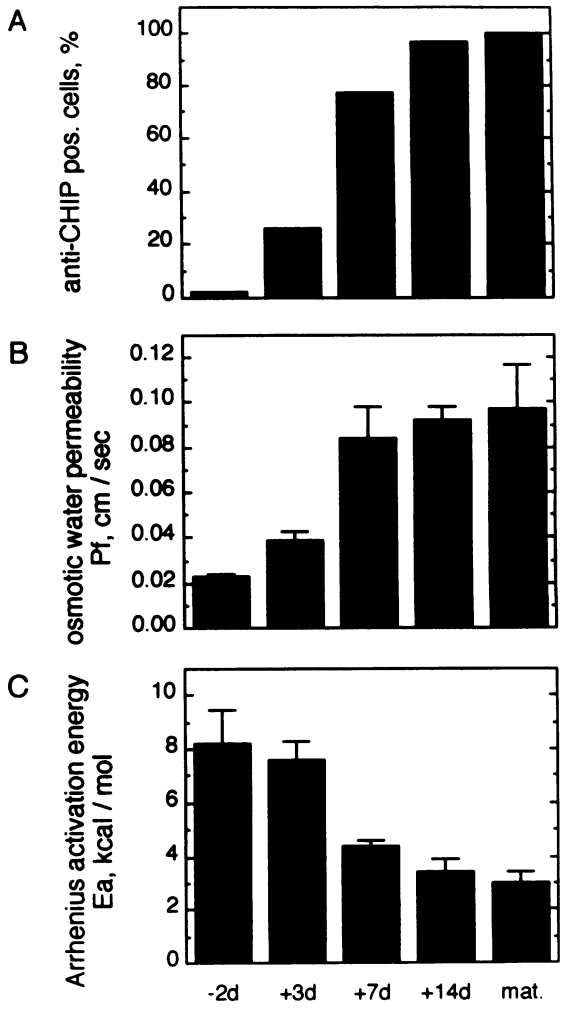

Figure 5. Concurrent expression of aquaporin CHIP, osmotic water permeability, and Arrhenius activation energy in red cells from rats of defined ages. (*A*) The percentage of permeabilized red cell membranes visualized with anti-CHIP (FITC) compared with the total number of red cells visualized with antispectrin (Texas red). From 300 to 1,000 cells were counted in each group. (*B*) Osmotic water permeability determined at 23°C on red cells from rats of defined ages (mean±SD, $n = 3$). Red cell samples from −2- and +3-d rats each differed from the mature samples, $P < 0.05$ (one-way analysis of variance and bonferroni t tests). (*C*) Activation energies derived from slopes of the Arrhenius plots (Fig. 4 *C*) of the measurements on the same samples performed at 9–39°C.

The apparent lack of CHIP before day +3 is not likely the result of proteolysis. CHIP within the lipid bilayer is relatively resistant to proteases (5), and identical immunoblots were generated by using affinity-purified anti-CHIP antibody specific for the COOH-terminal 4-kD domain (Fig. 2) or an affinity-purified antipeptide antibody corresponding to the protease-resistant NH_2 terminus (not shown). Moreover, when these membranes were analyzed for the presence of spectrin or ankyrin (not shown) or anion exchanger-band 3 (Fig. 2), the red cell membranes of prenatal, postnatal, and mature rats exhibited similar patterns.

Red cell membranes were examined for the presence of CHIP by flow cytometry with anti-CHIP and compared with nonimmune IgG (Fig. 3, *top*). The prenatal membranes contained negligible anti-CHIP–positive cells. A small shoulder of anti-CHIP–positive cells was seen at postnatal day +3, and this grew larger and broader in the +7-d sample, consistent with the appearance of a heterogeneous group of anti-CHIP–positive cells. By day +14 the peak of anti-CHIP–positive cells was only slightly broader than the peak in the mature sample.

Inspection of fixed permeabilized red cell membranes was undertaken with a double immunofluorescence method designed to optically reveal anti-CHIP–positive red cells within a field in which all red cells were labeled with antispectrin (Fig. 3, *middle* and *bottom*). Red cell membranes from −2-d prenatal samples were only observed with the antispectrin (decorated with Texas red). A minor fraction of red cell membranes of the +3-d postnatal sample were observed with anti-CHIP (decorated with FITC). By postnatal day +7, most red cell membranes reacted with both antibodies, although the intensity of anti-CHIP staining was not uniform. By postnatal day +14, virtually all of the membranes were uniformly stained with anti-CHIP.

Osmotic water permeability of perinatal red cells. The physiological consequence of the lack of CHIP in prenatal and early postnatal red cells was evaluated by measuring cell shrinkage by light scattering after an abrupt increase in extracellular osmolality. When measured at 23°C, red cells from mature rats responded rapidly to the increased osmolality and reached equilibrium in < 200 ms (Fig. 4 *A*). In contrast, red cells from −2-d prenatal rats shrank more slowly, only reaching equilibrium after 1.5 s (Fig. 4 *B*). Similar experiments were performed between 9 and 39°C, and Arrhenius curves were calculated (Fig. 4 *C*). The red cells from mature animals exhibited a low Arrhenius activation energy (E_a = 3.0±0.4 kcal/mol), consistent with measured values of channel-mediated water transport (E_a < 6 kcal/mol) (reviewed by Solomon et al., reference 23). A significantly higher value was determined from the −2-d sample (E_a = 8.2±1.3 kcal/mol), consistent with diffusional water permeability. Nevertheless, it remains possible that a small number of water channels encoded by a distinct gene may be present in the prenatal red cells.

A correlation was established between the presence of CHIP and membrane water transport. Red cell membranes were obtained from −2-, +3-, +7-, and +14-d rat pups and mature animals. The fractions of anti-CHIP–positive cells (Fig. 5 *A*) were compared with the osmotic water permeabilities (Fig. 5 *B*) and the Arrhenius activation energies (Fig. 5 *C*). Red cells from −2-d rats contained negligible CHIP and exhibited low water permeability with high Arrhenius activation energy. Red cells from +14-d pups resembled red cells from mature rats. Samples from +3- and +7-d pups exhibited intermediate values. Although not directly established, the presence of CHIP may contribute to the greater longevity of mature red cells within the peripheral circulation.

Membrane lipid composition of perinatal red cells. Membrane phospholipid content and composition were determined to assess whether a major difference in lipid could account for the striking differences in water permeability. Only small differences were noted in the minor phospholipids (Table I), and these are not likely explanations for reduced water permeability (Figs. 4 and 5) or reduced filterability of fetal red cells (24), since other studies failed to detect differences in transmembrane water movement in proteoliposomes containing CHIP reconstituted with a variety of lipids (25).

Expression of aquaporin CHIP in perinatal rat kidney. The developing nephron is known to differentiate in four stages at the time of birth in rats (26, 27). Immunoblots of perinatal rat kidneys were not performed because of the inability to adequately remove red cells by perfusion, but a marked induction of renal CHIP expression was observed at this time by immunohistochemical staining with anti-CHIP (Fig. 6). 3 d before birth, CHIP was detectable in both apical and basolateral membranes of stage III and IV proximal tubules in cortex and descending thin limbs in medulla (Fig. 6). 2 d after birth, anti-CHIP immunostaining remained weak over stage III proximal

Table I. Phospholipid Composition of Red Cell Membranes

	Percent of total phospholipid			
	+2-d pups		Mature rats	
Lipid	Saturated	Unsaturated	Saturated	Unsaturated
Phosphatidylcholine	46	19	50	21
Phosphatidylethanolamine	2.6	14	10	13
Phosphatidylserine plus phosphatidylinositol	2.2	16	3.1	2.0
Total	51	49	63	36

Packed red cell membranes contained equivalent concentrations of spectrin estimated from Coomassie-stained SDS-PAGE slabs. Phospholipids were isolated and quantitated as described (20): 190 nmol of total phospholipid phosphorus per 100 μl red cell membranes prepared from +2-d pups; 148 nmol from mature rats. Component fatty acids were converted to methyl esters; ~475 ng (phosphatidylcholine or phosphatidylethanolamine) and 180 ng (phosphatidylserine plus phosphatidylinositol) were analyzed by capillary gas chromatography as described (20). Repeated analyses confirmed the distribution pattern for the major phospholipids (phosphatidylcholine) but some variability was noted among the minor species.

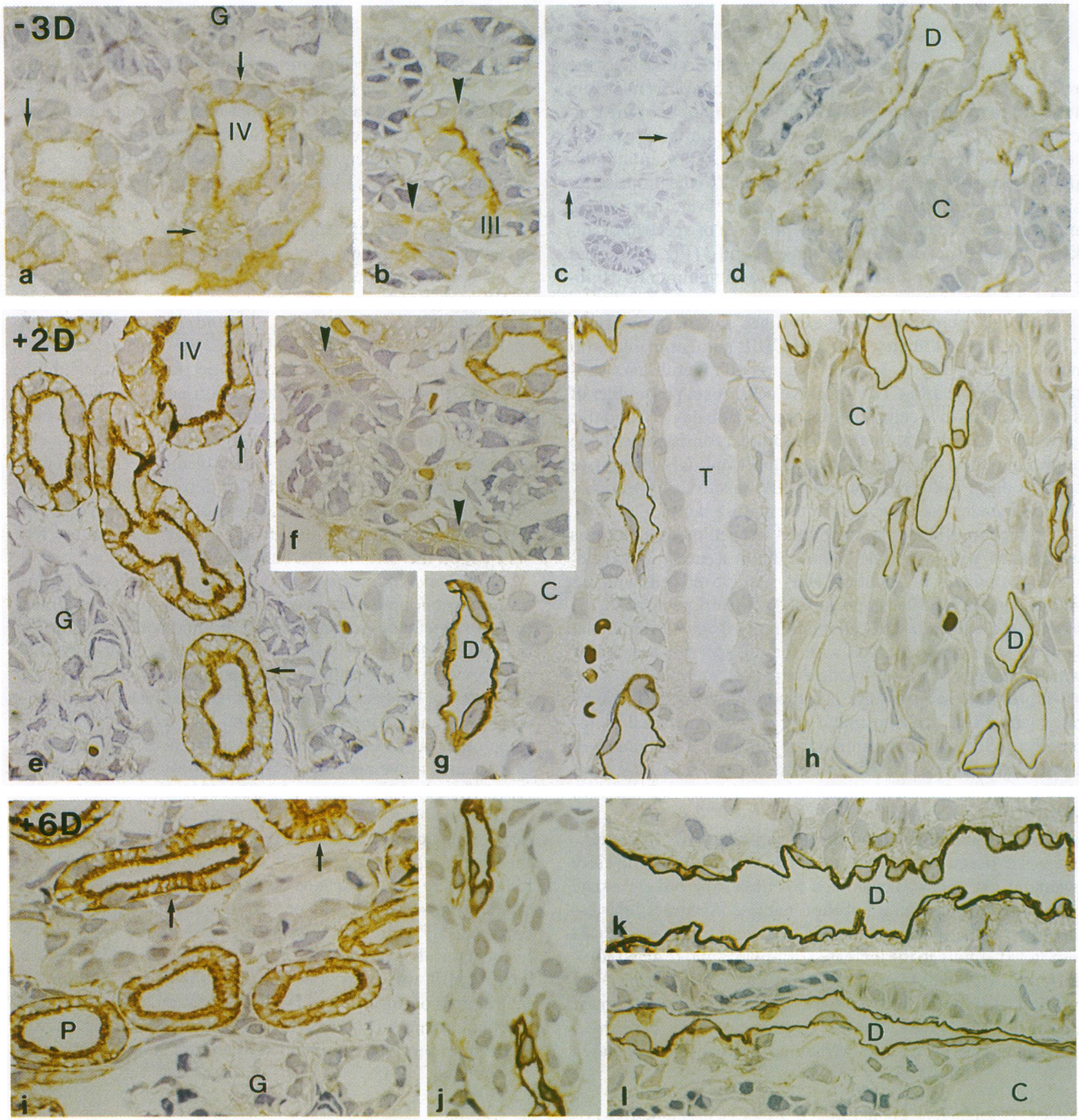

Figure 6. Immunohistochemical distribution of aquaporin CHIP in cortex and medulla of developing rat kidneys. (*a, b, c,* and *d*) 3 d before birth (*−3D*): (*a*) basolateral membranes (*arrows*) and apical membranes of stage IV proximal tubules exhibited detectable immunolabeling, but glomeruli (*G*) did not react with anti-CHIP; (*b*) stage III proximal tubules (*arrowheads*) had detectable immunolabeling; (*c*) neither stage III nor IV proximal tubules reacted with nonimmune IgG; (*d*) medullary descending thin limbs (*D*) exhibited detectable immunolabeling, whereas collecting ducts (*C*) did not react. (*e, f, g,* and *h*) 2 d after birth (*+2D*): (*e* and *f*) basolateral membranes (*arrows*) and apical membranes of stage IV proximal tubules reacted strongly with anti-CHIP, whereas stage III proximal tubules (*arrowheads*) exhibited relatively less immunolabeling, and glomeruli (*G*) did not react; (*g*) outer medullary and (*h*) inner medullary descending thin limbs (*D*) reacted strongly with anti-CHIP, whereas thick ascending limbs (*T*) and collecting ducts (*C*) did not. (*i, j, k,* and *l*) 6 d after birth (*+6D*): (*i*) proximal tubules (*P*) exhibited very strong immunolabeling of basolateral and apical membranes, including developed basolateral infoldings (*arrows*); (*j* and *k*) descending thin limbs (*D*) within inner stripe of outer medulla and (*l*) inner medulla reacted intensely with anti-CHIP. ×260 (*c*) or ×560 (*a, b,* and *d–l*).

tubules, but the immunostainings of apical and basolateral membranes of stage IV proximal tubules and the apical and basolateral membranes of descending thin limbs were all very strong. This expression pattern is consistent with the known expression of other apical proteins during assembly of the brush border in stage III proximal tubules (26, 27). Moreover,

the intensity of staining at apical and basolateral membranes was always equivalent, suggesting that the appearance of CHIP occurs simultaneously in both membranes. Consistent with studies of mature rat kidney (10), anti-CHIP immunostaining was not observed over thick ascending limbs, which are known to be water impermeable, and collecting ducts that contain the aquaporin WCH-CD (human genome symbol AQP2), the presumed vasopressin-regulated water channel (28). Postnatal expression of CHIP in erythroid and renal locations is specific, since the protein is expressed in choroid plexus, cornea, and at other locations throughout development (17).

As reported here, rat red cells lack the aquaporin CHIP or a fetal water channel isoform until after birth. CHIP is then expressed in red cells that acquire channel-mediated water permeability (Figs. 4 and 5). CHIP is concurrently expressed in the proximal nephron and descending thin limbs of Henle's loop, where the protein facilitates reabsorption of ~ 90% of the glomerular filtrate, permitting successful operation of the countercurrent multiplier (10). By increasing water permeability of the proximal tubule and descending thin limb, CHIP plays an essential role in this renal concentration mechanism, and rat kidneys are known to begin concentrating soon after birth (29). Concurrent, perinatal expression strongly supports the hypothesis that red cell water channels exist to permit rapid rehydration of red cells after transit through the renal medulla, which becomes markedly hypertonic after birth. This hypothesis resembles the theoretical need proposed for urea transport (30).

The relevance of these studies to human erythroid and renal development remains to be established. Although expression of CHIP is reminiscent of the globin switching phenomenon described in the human fetus, rodents do not express a fetal globin, so induction of both proteins is not linked. Nevertheless, preliminary studies revealed that red cells of full-term human infants are not deficient in CHIP, but induction appears early in the third gestational trimester (Baumgarten, R., and P. Agre, unpublished results). This is consistent with the hypothesis proposed here, since human kidneys are far more developed at birth than are rat kidneys. Definitive studies of human aquaporin CHIP expression are underway.

Acknowledgments

We thank Linda Smith, Vicky Flanigan, Peggy Beverungen, H. Sidelmann, I. Kristoffersen, Matt Jarpe, and Gordon Wiegand for excellent technical assistance, and Carolyn Machamer for scientific suggestions and use of her microscope.

Support for this study was provided by National Institutes of Health grants HL-33991, HL-48268, HL-39086, and DK-43955; the Danish Medical Research Council; the Biomembrane Research Center and Research Foundation of the University of Aarhus; and the Novo Foundation. R. Baumgarten was supported by the medical student exchange program between Erasmus University, Rotterdam, and Johns Hopkins University. M. L. Zeidel received Career Development and Merit Review Awards from the Veterans Administration.

References

1. Matovcik, L. M., and W. C. Menzer. 1985. The membrane of the human neonatal red cell. *Clin. Haematol.* 14:203–221.

2. Oski, F. A. 1993. The erythrocyte and its disorders. *In* Hematology of Infancy and Childhood, 4th ed. D. G. Nathan and F. A. Oski, editors. W. B. Saunders Company, Philadelphia. 18–43.

3. Barton, T. C., and D. A. J. Brown. 1964. Water permeability of the fetal erythrocyte. *J. Gen. Physiol.* 47:839–849.

4. Denker, B. M., B. L. Smith, F. P. Kuhajda, and P. Agre. 1988. Identification, purification, and characterization of a novel M_r 28,000 integral membrane protein from erythrocytes and renal tubules. *J. Biol. Chem.* 263:15634–15642.

5. Smith, B. L., and P. Agre. 1991. Erythrocyte M_r 28,000 transmembrane protein exists as a multi-subunit oligomer similar to channel proteins. *J. Biol. Chem.* 266:6407–6415.

6. Preston, G. M., and P. Agre. 1991. Molecular cloning of the red cell integral membrane protein of M_r 28,000: a member of an ancient channel family. *Proc. Natl. Acad. Sci. USA.* 88:11110–11114.

7. Preston, G. M., T. P. Carroll, W. B. Guggino, and P. Agre. 1992. Appearance of water channels in *Xenopus* oocytes expressing red cell CHIP28 protein. *Science (Wash. DC).* 256:385–387.

8. Agre, P., S. Sasaki, and M. J. Chrispeels. 1993. Aquaporins: a family of water channel proteins. *Am. J. Physiol.* 265:F461.

9. Zeidel, M. L., S. V. Ambudkar, B. L. Smith, and P. Agre. 1992. Reconstitution of functional water channels in liposomes containing purified red cell CHIP28 protein. *Biochemistry.* 31:7436–7440.

10. Nielsen, S., B. L. Smith, E. I. Christensen, M. Knepper, and P. Agre. 1993. CHIP28 water channels are localized in constitutively water-permeable segments of the nephron. *J. Cell Biol.* 120:371–383.

11. Agre, P., G. M. Preston, B. L. Smith, J. S. Jung, S. Raina, C. Moon, W. B. Guggino, and S. Nielsen. 1993. Aquaporin CHIP, the archetypal molecular water channel. *Am. J. Physiol.* In press.

12. Moon, C., G. M. Preston, C. Griffin, E. W. Jabs, and P. Agre. 1993. The human aquaporin CHIP gene: structure, organization, and chromosomal localization. *J. Biol. Chem.* 268:15772–15778.

13. Lanahan, A., J. B. Williams, L. K. Sanders, and D. Nathans. 1992. Growth factor-induced delayed early response genes. *Mol. Cell. Biol.* 12:3919–3929.

14. Deen, P. M. T., J. A. Dempster, B. Wieringa, and C. H. Van Os. 1992. Isolation of a cDNA for rat CHIP28 water channel: high mRNA expression in kidney cortex and inner medulla. *Biochem. Biophys. Res. Commun.* 188:1267–1273.

15. Nielsen, S., B. L. Smith, E. I. Christensen, and P. Agre. 1993. Distribution of the Aquaporin CHIP in secretory and resorptive epithelia and capillary endothelia. *Proc. Natl. Acad. Sci. USA.* 90:7275–7279.

16. Finkelstein, A. 1987. Water movement through lipid bilayers, pores, and plasma membranes, theory and reality. John Wiley & Sons, Inc., New York. 153–183.

17. Bondy, C., E. Chin, B. L. Smith, G. M. Preston, and P. Agre. 1993. Developmental gene expression and tissue distribution of the CHIP28 water channel. *Proc. Natl. Acad. Sci. USA.* 90:4500–4504.

18. Bennett, V. 1983. Proteins involved in membrane-cytoskeleton association in human erythrocytes: spectrin, ankyrin, and band 3. *Methods Enzymol.* 96:313–324.

19. Laemmli, U. K. 1970. Cleavage of structural proteins during the assembly of the head of bacteriophage T4. *Nature (Lond.).* 227:680–685.

20. Doering, T. L., M. S. Pessin, E. F. Hoff, G. W. Hart, D. M. Raben, and P. T. Englund. 1993. Trypanosome metabolism of myristate, the fatty acid required for the variant surface glycoprotein membrane anchor. *J. Biol. Chem.* 268:9215–9222.

21. Larsson, L. 1975. Effects of different fixatives on the ultrastructure of the developing proximal tubule in rat kidney. *J. Ultrastruct. Res.* 51:140–151.

22. Fukuda, M., A. Dell, and M. N. Fukuda. 1984. Structure of fetal lactosaminoglycan. *J. Biol. Chem.* 259:4782–4791.

23. Solomon, A. K., B. Chasan, J. A. Dix, M. F. Lukacovic, M. R. Toon, and A. S. Verkman. 1983. The aqueous pore in the red cell membrane. *Ann. NY Acad. Sci.* 414:97–124.

24. Colin, F. C., Y. Gallois, D. Rapin, A. Meskar, J.-J. Chabaud, M. Vicariot, and J.-F. Menez. 1992. Impaired fetal erythrocytes' filterability: relationship with cell size, membrane fluidity, and membrane lipid composition. *Blood.* 79:2148–2153.

25. Zeidel, M. L., B. L. Smith, S. Ambudkar, and P. Agre. 1993. Properties of reconstituted CHIP28 water channels: channel selectivity and role of the carboxy-terminal domain. *Clin. Res.* 41:186*a*. (Abstr.)

26. Biemesderfer, D., G. Dekan, P. S. Aronson, and M. G. Farquhar. 1992. Assembly of distinctive coated pit and microvillar microdomains in the renal brush border. *Am. J. Physiol.* 262:F55–F67.

27. Aperia, A., and G. Celsi. 1992. Ontogenic processes in nephron epithelia: structure, enzymes, and function. *In* The Kidney: Physiology and Pathophysiology, 2nd ed. D. W. Seldin and G. Giebisch, editors. Raven Press, Ltd., New York. 803–828.

28. Fushimi, K., S. Uchida, Y., Hara, Y. Hirata, F. Marumo, and S. Sasaki. 1993. Cloning and expression of apical membrane water channel of rat kidney collecting tubule. *Nature (Lond.).* 361:549–552, 1993.

29. Rane, S., A. Aperia, P. Eneroth, and S. Lundin. 1985. Development of urinary concentrating capacity in weaning rats. *Pediatr. Res.* 19:472–475.

30. Macey, R. I., and L. W. Yousef. 1988. Osmotic stability of red cells in renal circulation requires rapid urea transport. *Am. J. Physiol.* 254:C669–C674.